Biogeochemistry (2021) 154:119–138
https://doi.org/10.1007/s10533-021-00801-y

# Differential subsurface mobilization of ambient mercury and isotopically enriched mercury tracers in a harvested and residue harvested hardwood forest in northern Minnesota

**Colin P. R. McCarter · Stephen D. Sebestyen · Susan L. Eggert · Randall K. Kolka · Carl P. J. Mitchell**

Received: 30 January 2021 / Accepted: 21 April 2021 / Published online: 29 April 2021


**Abstract** Mercury is a global pollutant of critical concern but its movement through terrestrial upland systems is poorly understood. We investigated whether forest harvesting practices and varying hydrological conditions resulted in different subsurface transport pathways, fluxes and proportions of recent vs. ambient mercury in runoff. In a multiyear field experiment, we measured subsurface lateral mercury fluxes at three adjacent hillslope plots, including one that was not harvested, one where all biomass was removed after harvest, and one where residual biomass was left after harvest. Two different enriched stable mercury isotopes (Hg tracer) were added to the hillslope plots (one pre-harvest and one post-harvest) to help differentiate between recently deposited mercury and ambient mercury in soils, as well as to identify changes between years. More Hg tracer was recovered in runoff post-harvest (16.2–54.0 µg) than pre-harvest (3.7–11.8 µg) from both harvested hillslopes, but differences between harvested hillslopes were not significant. The movement of Hg tracer was governed by periods of near surface preferential flow that was enhanced by forest harvesting. Runoff Hg tracer concentrations were significantly and inversely related to both event runoff magnitude ($R^2$ = 0.85) and runoff ratio ($R^2$ = 0.81). Insignificant relationships between Hg tracer concentrations and both DOC and precipitation pH suggest that for recently deposited mercury, the overarching controls on mobilization were hydrological rather than biogeochemical. The dependence of mercury mobilization on the routing of precipitation to different subsurface flow pathways suggests an important interaction between climate and the age of mercury pools for mercury transport from terrestrial landscapes.

**Keywords** Mercury · Biomass harvest · Soil · Dissolved organic carbon · Silviculture · Throughflow

Responsible Editor: James Sickman

**Supplementary Information** The online version contains supplementary material available at https://doi.org/10.1007/s10533-021-00801-y.

C. P. R. McCarter · C. P. J. Mitchell (✉)
Department of Physical and Environmental Sciences, University of Toronto Scarborough, 1265 Military Trail, Scarborough, ON M1C 1A4, Canada
e-mail: carl.mitchell@utoronto.ca

S. D. Sebestyen · S. L. Eggert · R. K. Kolka
USDA Forest Service Northern Research Station, Grand Rapids, MN 55744, USA

## Introduction

Forest disturbances can intensify downstream contaminant loading through changes in hydrology, organic carbon dynamics and erosion (Bishop et al.

2009; Devito et al. 2000; Hsu-Kim et al. 2018; Kreutzweiser et al. 2008). The terrestrial landscape is generally a large, long-term sink for atmospherically deposited mercury. When forests are disturbed, such as through harvesting, mercury is more susceptible to mobilization and potentially down-gradient bioaccumulation (Eklöf et al. 2016; Hsu-Kim et al. 2018). Nonetheless, the extent to which mercury is mobilized from catchments is oftentimes unclear due to climatic variability (Oswald and Branfireun 2014), the large capacity of soil organic matter to bind inorganic mercury (Hintelmann et al. 2002; Oswald et al. 2014), and a general lack of the quantification of processes that affect mercury transport through forested systems and soils.

Approximately 6.5 million ha year$^{-1}$ of forests are harvested in North America (Masek et al. 2011). Forest harvesting may increase both inorganic and organic mercury (methylmercury) concentrations and downstream total loads (Bishop et al. 2009; Eklöf et al. 2016, 2018; Porvari et al. 2003; Ukonmaanaho et al. 2016), though empirical observations are not always consistent (Eklöf et al. 2016; Hsu-Kim et al. 2018). The post-harvest response in mercury mobilization depends on interactions and feedbacks among several hydrological, climatological, geomorphological, and biogeochemical processes and their associated responses to forest harvesting (Eklöf et al. 2014; Laudon et al. 2016; Porvari et al. 2003; Sørensen et al. 2009). These interactions are complicated by harvesting practices, such as residual biomass harvesting (*e.g.*, as renewable fuels; Janowiak and Webster 2010), which can differentially alter runoff generation (Holub et al. 2013; McCarter et al. 2020a) and biogeochemical processes (Laurén et al. 2008; Oni et al. 2015; Pinel-Alloul et al. 2002; Schelker et al. 2012) governing mercury mobilization relative to leaving residual biomass (*i.e.* harvest slash) onsite. Many studies of forest management and mercury mobilization focus on cumulative impact in catchments (Bishop et al. 2009; Eklöf et al. 2014; Kronberg et al. 2016; Porvari et al. 2003). Studies at smaller scales, such as hillslopes, that are conducive to elucidating mechanisms of mercury mobilization are rare.

Enriched stable mercury isotope additions may serve as a means of tracing more recently deposited mercury in experimental studies (Harris et al. 2007). When combined with hydrological studies, enriched stable mercury isotope tracers offer the potential to provide further insight into mercury mobilization processes (Gai et al. 2016; Harris et al. 2007; Haynes and Mitchell 2015; Hintelmann et al. 2002; Oswald et al. 2014). For example, periods of high wetland water tables led to accelerated subsurface transport of surficially-added enriched stable mercury isotope tracers (Branfireun et al. 2005). In a forested upland, Hintelmann et al. (2002) observed a small pulse of enriched stable mercury isotope tracer in runoff linked to a precipitation event soon after application, with little tracer observed thereafter. In the multi-year and loading-focused METAALICUS study, Harris et al. (2007) observed that enriched stable mercury isotope tracers from terrestrial areas also contributed only small amounts of mercury ($\sim$ 1%) in runoff entering a lake. At the laboratory scale, both Gai et al. (2016) and Haynes and Mitchell (2015) investigated the transport of inorganic mercury under unsaturated conditions, though these studies may not represent the bulk transport of mercury under field conditions that has been linked to increases in water table elevations (Hintelmann et al. 2002; Oswald et al. 2014). In all of these studies (Gai et al. 2016; Haynes and Mitchell 2015; Hintelmann et al. 2002), mercury export (both ambient and tracer) has been correlated to dissolved organic carbon (DOC) concentrations, suggesting that dissolved organic matter (DOM) is a key ligand in the transport of different mercury pools on the landscape.

Jiskra et al. (2017) highlighted the potential for the differential mobility of unique mercury pools within a landscape by observing that proportionally more mercury was associated with near-surface soil DOC than deeper soil DOC in a stream draining a boreal forest in Sweden. Regardless of harvesting, mercury mobilization is also dependent on flow path generation (Porvari et al. 2003), but linkages between particular hydrological processes and mercury mobilization remain unclear in both unmanaged and managed forests. Understanding these linkages is critical to properly assessing whether climate change will impact the mobilization of different mercury pools in forests, particularly as the deposition of atmospheric mercury declines (Bishop et al. 2020). The objectives of this study, therefore, were to: (1) test whether forest harvesting, and subsequent biomass removal increase the mobilization of more recently deposited (*e.g.*, within one year of deposition) vs. legacy mercury pools by using field-level additions of enriched

stable isotope mercury tracers, (2) examine relationships between mercury pools, DOC, and (3) elucidate mechanisms governing the mobilization of different mercury pools from forested and forest-harvested hillslopes.

## Methods

### Study site

The study was conducted from 2010 through 2013 in north-central Minnesota, USA on a north-facing hillslope in the S7 catchment at the USDA Forest Service's Marcell Experimental Forest (MEF) (47°31′N, 93°28′W). The climate at the MEF is sub-humid continental with an average daily temperature of 3.4 °C (average temperatures of 13.9 °C during the months of April to September and − 5.6 °C for the months of October to March) (Sebestyen et al. 2011). Mean annual precipitation for the MEF is 787 mm (Sebestyen et al. 2021b), of which ~ 420 mm is rainfall between April and October (Verry et al. 2018). The upland overstory vegetation in the S7 catchment is predominately sugar maple (*Acer saccharum*), trembling aspen (*Populus tremuloides*) and paper birch (*Betula papyrifera*). Tree density and forest composition was similar across the entire hillslope prior to harvest.

The hillslope has a mean slope of 18°. A thin (~ 50 cm) permeable sandy loam with a shallow organic layer (generally < 2 cm) overlies a low permeability confining layer of Koochiching clay loam till (Fig. 1) (Mitchell et al. 2009; Verry et al. 2011). Hillslope runoff generation is predominantly as shallow throughflow above the Koochiching clay loam till (McCarter et al. 2020a; Timmons et al. 1977; Verry and Timmons 1982). Haynes and Mitchell (2012) determined the vertical distribution of ambient mercury mass in the soil was 1.5 ± 0.5, 0.8 ± 0.3 and 2.5 ± 0.3 mg $m^{-2}$, for soil layers 0 to 7.5, 7.5 to 15, and 15 to ~ 50 cm below the ground surface, respectively. Soil organic carbon rapidly decreases with depth from 4% loss on ignition in the 0 to 7.5 cm layer to ~ 1% further down in the sandy loam soil profile (Haynes and Mitchell 2012).

### Experimental design

The overall experimental approach in this study was a hillslope-scale harvesting experiment using the Before-After-Control-Impact (BACI) design (*e.g.*, Stewart-Oaten et al., 1986). The S7 hillslope was divided into three ~ 20 m wide by ~ 55 m long (downslope) experimental hillslope plots including (1) a plot that was clearcut and the majority of residual biomass harvested (Biomass Removed hillslope), (2) a plot that was clearcut with substantial residual biomass left (Biomass Left hillslope), and (3) a plot that was left unharvested (Unharvested Control hillslope) (Fig. 1). The Biomass Left and Biomass Removed hillslopes were machine-harvested in March 2012 under snow-covered, frozen ground conditions. At the Biomass Removed hillslope, large residual biomass was machine-harvested and small diameter wood was manually removed, resulting in ~ 85% of all residual biomass removed from the hillslope (Mazur et al. 2014). The harvest blocks spanned from the toe of slope to above the top of the hillslope (Fig. 1). Measurements and sampling were from 2010 through 2013, constituting a 2-year pre-harvest period in 2010 and 2011 followed by a 2-year post-harvest period in 2012 and 2013. We focus here on hillslope runoff fluxes resulting from field additions of two isotopically enriched mercury tracers from April-November in 2011 and 2012. The site and experimental setup have been the subject of other related studies, including Mazur et al. (2014) regarding surface-atmosphere mercury exchanges and McCarter et al. (2020a) regarding changes in hydrological processes.

A shallow subsurface runoff trench and water collection system was constructed at the toe of the hillslope of each of the three experiment plots in 2009 to quantify the magnitude of upland runoff reaching an adjacent peatland (Fig. 1). Water infiltration into the soil within ~ 1 m upslope and directly on the subsurface runoff trenches was excluded. Throughflow runoff volume was measured every 15 min using tipping bucket flow meters at the outlet of each runoff trench. Contributing areas to each trench were calculated based on the topography of the relatively impermeable Koochiching clay loam till layer that is found below the upper 15–146 cm (avg. 55 ± 31 cm) loess sandy loam horizon in which throughflow occurs. The topography of the clay loam till layer was mapped via a fine-resolution surface digital

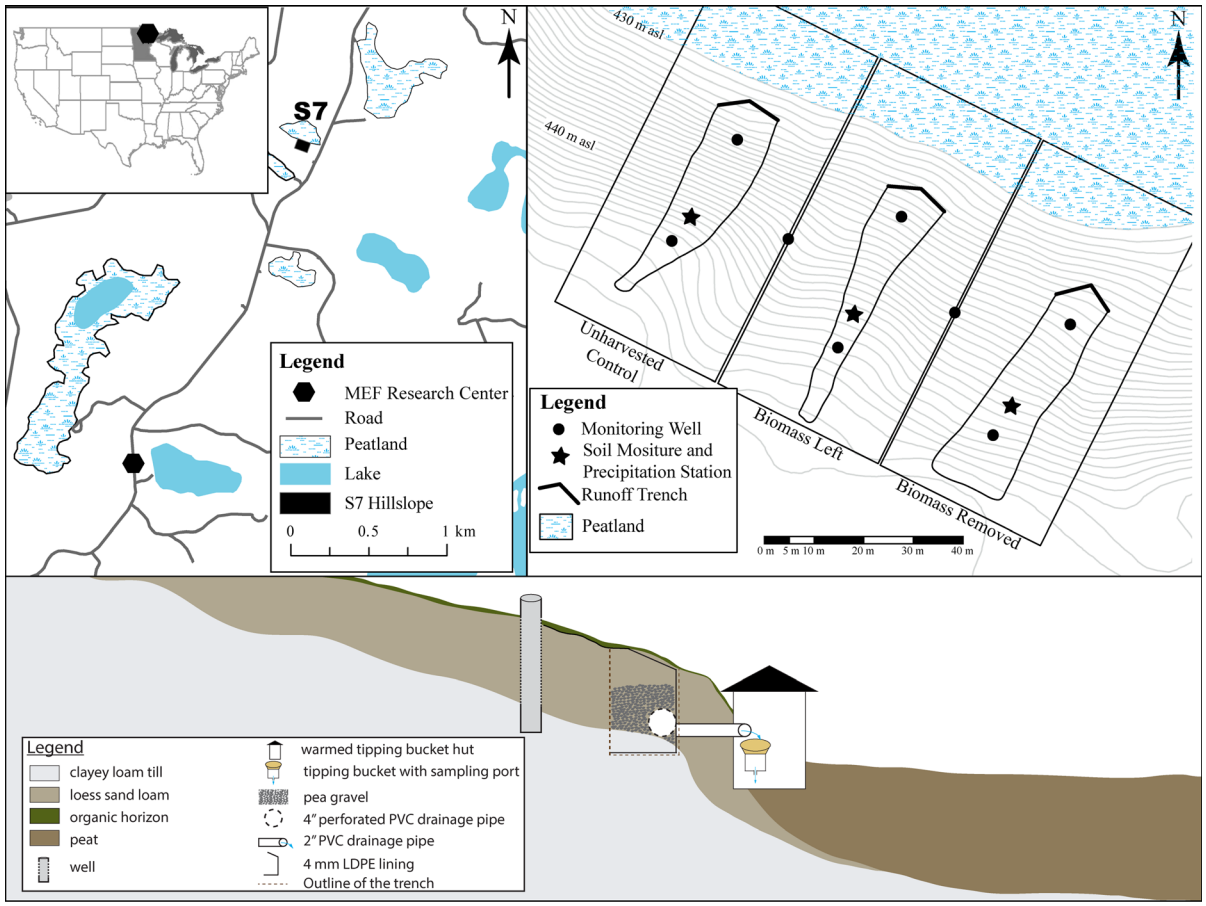


**Fig. 1** (Top) Location and map of study site and monitoring equipment. (Bottom) A schematic of the runoff trench, monitoring well and hillslope topography. Adapted from McCarter et al. (2020a)

elevation model (DEM) overlain on a detailed soil depth survey (Haynes and Mitchell 2012). A thin organic horizon (generally $< 2$ cm) overlies the sandy loam with little year-to-year persistence (Hale et al. 2005) (Fig. 1). The catchment areas of each runoff trench were well within the bounds of each harvest block (Fig. 1). The water table of the sandy loam aquifer, which was perched above the Koochiching clay loam till, was measured directly above the runoff trenches and at the top of slope using pressure transducers measuring every 15 min (McCarter et al. 2020a). Hillslope overland flow is rare in the MEF landscape accounting for $\sim$ 10% of runoff (Kolka et al. 2001; Sebestyen et al. 2021a) though overland flow was never observed at the study site (McCarter et al. 2020a).

## Mercury tracer application

Two different mercury tracers (94.3% enriched $^{200}$Hg during 2011 and 42.1% enriched $^{204}$Hg during 2012 (both from Trace Sciences International) were applied to the surface of the entire S7 hillslope during light spring precipitation events on May 3rd and 4th in 2011 and May 13th, 2012 with a target deposition of 14 μg m$^{-2}$. The two tracers were used to help differentiate the behavior of recently deposited mercury, as represented by the enriched stable mercury isotopes (Harris et al. 2007), from the ambient mercury soil pool, as well as to identify changes between years. We note that the targeted deposition rate is based on a well-characterized history of Hg wet deposition in the area, though more recently, Hg dry deposition has been demonstrated to be a major input toward Hg accumulation in forest soils (Zhou et al.

2021). We were particularly interested in the inter-annual variability of recent mercury deposition in runoff and whether the transport mechanisms of recently deposited mercury were the same as those for ambient mercury. Although the preparation of isotopes was similar, our focus on tracing transport pathways differs from the foundational field applied enriched stable mercury isotope METAALICUS study (Harris et al. 2007), which was a study of longer-term loading of enriched stable mercury isotopes.

The preparation of enriched stable isotope solutions closely followed previous protocols used in the METAALICUS study (Harris et al. 2007; Hintelmann et al. 2002). Our stock isotope solutions were preserved in HCl, presumably as $HgCl_2$. Application solutions were mixed in polyethylene backpack-mounted sprayers. Enough of the stock isotope solution was added to 18 L of pH adjusted water (pH = 5.4; adjusted using a trace metal grade sulfuric-nitric acid mixture) in each sprayer reservoir. When sprayed evenly on a 650 $m^2$ area per sprayer, the resulting deposition equaled $\sim$ 10.5 μg $m^{-2}$ of enriched tracer each year to the ground surface (Mazur et al. 2014). This deposition rate was $\sim$ 25% below our target enriched tracer due to losses during spraying (Ericksen et al. 2005). Three researchers wearing the sprayers simultaneously applied the isotope solutions under low sunlight and lightly raining conditions. The addition of the enriched tracer was excluded from $\sim$ 3 m upslope of the subsurface runoff trenches. The addition of enriched stable isotope mercury was therefore approximately equal to the average 2009–2018 (latest 10 years available) annual atmospheric wet deposition (7.0 μg $m^{-2}$) (National Atmospheric Deposition Program (MN16) 2021).

Herein, we simplify "enriched stable mercury isotope" to "mercury tracer" when referring to both enriched stable inorganic mercury isotopes [*i.e.*, $^{200}$Hg(II) or $^{204}$Hg(II)]. As pointed out in the chemical analysis section and because of our use of enriched isotopes, "mercury tracer" accounts for the amount of $^{200}$Hg(II) or $^{204}$Hg(II) that is in excess of its natural abundance. When needed, we specify a given enriched stable mercury isotope, for instance, when comparing the mobility of the enriched stable mercury isotope between the two study years. The mercury in the system, not represented by the addition of the enriched stable isotope mercury (mercury tracer), is referred to as "ambient mercury".

## Water sampling

Water in runoff was sampled on both an event and regular interval basis. We focused considerable sampling effort within the snowmelt period of each year (March–April) because this period usually represents the highest flows and a disproportionately high amount of the annual mercury load from catchments in the area (Mitchell et al. 2009). At each runoff collector, we sampled 1–3 times per day during the snowmelt periods. Outside of the snowmelt period, we sampled weekly to bi-weekly until freeze-up in early November, except when runoff ceased during drier, mid-summer conditions. When possible, regular sampling was augmented with event-based sampling during or shortly following rainfall events throughout the spring, summer, and fall.

Ultra-trace sampling protocols were used (EPA Method 1669). Samples for mercury analyses were collected in polyethylene tetraglycol (PETG) bottles, preserved via the addition of 0.5% by volume trace metal-grade HCl, and stored cold and in the dark in double zip-sealed plastic bags. All other chemical constituents were sampled into high-density polyethylene bottles and refrigerated until analysis. All water samples were filtered through pre-ashed 0.7 μm glass microfiber filters.

## Chemical analysis

Total mercury (THg) in water was analyzed with a Tekran 2600 automated mercury analysis system (cold vapour dual gold trap amalgamation system), which was hyphenated directly to an Agilent 7700 inductively coupled plasma mass spectrometer (ICP-MS) to quantify mercury isotope ratios. Quantification of "excess" isotope mercury (the amount in each sample that can be directly attributed to the added enriched isotope because of its deviation from natural isotope abundance ratios) was based on a matrix of isotope ratio calculations according to the methods of Hintelmann and Ogrinc (2002). We used the dominant natural isotope $^{202}$Hg, compensated for its quantity in the applied isotopes, for calculations of ambient THg concentration simultaneous to calculations of excess mercury isotope (tracer) content. Analytical precision (mean relative standard deviation of replicate samples) was 2.0% for ambient THg, 6.3% for excess $T^{200}$Hg and 3.8% for excess $T^{204}$Hg. Spike recoveries

for THg in water were 96 ± 8%. Method detection limits were 0.20 ng $L^{-1}$ for ambient THg, 0.03 ng $L^{-1}$ for excess $T^{200}Hg$ and 0.01 ng $L^{-1}$ for excess $T^{204}Hg$.

Dissolved organic carbon (DOC) concentrations (filtered at 0.7 µm, detection limit = 1 mg carbon $L^{-1}$) were measured as non-purgeable organic carbon by high-temperature combustion (Shimadzu TOC V-CPH, Standard Method 5310-C, APHA 2017) using potassium hydrogen phthalate (KHP) for reference and check standards (McCarter et al. 2021; Sebestyen et al. 2017). All reference and check standard were within 10% of the reported value. Weekly average precipitation values were from the NADP MN16 location [National Atmospheric Deposition Program (MN16) 2020]. See National Atmospheric Deposition Program (MN16) (2020) for further methodological details.

## Mercury loads

The mercury loads in subsurface hillslope runoff were determined as,

$$Hg_{load} = Q \cdot Hg_{conc} \quad (1)$$

where $Hg_{load}$ is the total load of mercury for a given mercury species (µg $day^{-1}$), $Q$ is the total daily runoff (L $day^{-1}$), and $Hg_{conc}$ is the average concentration of a given mercury species taken between two sampling points (µg $L^{-1}$). If measured $Q$ coincided with a $Hg_{conc}$ measurement, then the measured $Hg_{conc}$ value was used in the calculation of the $Hg_{load}$. Given the short time between samples, typically $< 10$ days, no time-weighted averaging was used. However, if the time between measurements was $> 10$ days and the runoff fell to zero at any point in that time period, the load calculation assumed a break in the continuous flow and the first $Hg_{conc}$ and subsequent values during the period of resumed flow was used to calculate the $Hg_{load}$.

Inter-annual variability in the total mass of mercury mobilized, along with change in precipitation and runoff efficiency (McCarter et al. 2020a), can mask changes in the mobilization of different mercury pools. To assess the mobility of the mercury tracer relative to the ambient mercury, the proportion of ambient mercury to the total measured mercury was determined by,

$$P_{amb} = \frac{Hg_{amb}}{Hg_{amb} + Hg_{tracer}} \quad (2)$$

where $P_{amb}$ was the proportion of ambient mercury relative to the total measured mercury for a given sample, $Hg_{amb}$ was the ambient mercury load (µg $day^{-1}$), $Hg_{tracer}$ was the "excess" load of either the tracer $^{200}Hg$ or $^{204}Hg$ (µg $day^{-1}$) for a given year (i.e., $^{200}Hg$ for 2011 and $^{204}Hg$ for 2012–2013).

## Hydrological measurements

Hydrological measurements were reported by McCarter et al. (2020a) for both study years on all hillslopes. Briefly, in each runoff trench the total subsurface discharge was measured using large tipping-bucket style flow meters housed in a heated wooden shelter and the runoff (mm) was determined by the contributing areas for each runoff trench determined by Haynes and Mitchell (2012). Bulk precipitation was measured at the nearby (~ 1 km south) MEF station (south_PCP) (Sebestyen et al. 2020). The event runoff ratio ($RR_e$), a measure of the hydrological connectivity of the hillslope, was determined by,

$$RR_e = \frac{R_e}{P_e} \quad (3)$$

where $R_e$ (mm) is the total event runoff and $P_e$ (mm) is the total event precipitation (McCarter et al. 2020a). A runoff event was determined from the start of runoff until the daily change in runoff was below 0.1 mm $day^{-1}$. The water table was continuously measured a few meters upslope of the apex of each runoff trench and used to calculate the change in water table from pre-event to the maximum water table for a given runoff event (McCarter et al. 2020a). The average proportion of the sandy loam aquifer that was saturated during each runoff event was estimated based on the measured water table near each runoff trench. The hydraulic gradient from the top of slope to the toe of slope (*i.e.*, directly upslope of the runoff trenches) was determined for each runoff event using surveyed wells and digitally recorded water elevations in each. The event average effective hydraulic conductivity was calculated using Darcy's Law with measured hydraulic parameters of runoff and hydraulic gradient. Soil moisture was measured mid-slope (Fig. 1), in the sandy loam, 5 cm above the

Koochiching clay loam till. For more details on the hydrological measurements and data see McCarter et al. (2020a) and McCarter et al. (2020b).

### Statistical analysis

All statistical analysis was performed in R Statistical Software (R Development Core Team 2021). Correlations between different runoff event hydrological and chemical measurements [average DOC concentration, total event runoff, event runoff ratio, proportion of saturated aquifer, total runoff event precipitation, change in water table, weekly average precipitation pH from the NADP MN16 location (National Atmospheric Deposition Program (MN16) 2020]) to the average event mercury tracer concentration were tested (alpha = 0.05) using linear regression. If the total runoff event precipitation fell on two weeks, the average of the weekly pH values was used. Additionally, the relationship between DOC concentration and mercury concentrations (both ambient and tracer) were evaluated using linear regression. Ambient THg–DOC relationships were determined for pre- (2010 and 2011) and post-harvest (2012 and 2013), while both enriched mercury isotope tracers ($^{200}$Hg for 2011 and $^{204}$Hg for 2012–2013) were pooled to increase sample size for the generation of a single linear regression with DOC, particularly for $^{200}$Hg, which typically had $< 3$ samples per site above the detection limit. The logarithm, either $\log_e$ or $\log_{10}$ depending on the specific analysis, of both dependent and independent parameters was taken to linearize the bivariate relationships from a 2-variable power function.

To assess the effect of harvesting practices on the mobilization of the different mercury pools a Before-After-Control-Impact design was used and each measurement of $P_{amb}$ at the treatment sites (Biomass Removed and Biomass Left hillslopes) was normalized to the corresponding temporal measurement from the Unharvested Control hillslope by determining the treatment ratio (TR) (Conner et al. 2016).

$$TR = \frac{TreatmentP_{amb}}{UnharvestedP_{amb}} \quad (4)$$

The natural logarithm TR was then used as the dependent variable in mixed effect models using the lmer function in the emmeans package (Lenth 2020),

$$\log_e(TR) = per * tre + (1|Date) \quad (5)$$

where *per* is the treatment period (pre- or post-harvest), *tre* is the treatment site (either Biomass Removed or Biomass Left) and *Date* is the date of measurement. The resultant least-squares means were then compared using the post-hoc Tukey test in the emmeans package (Lenth 2020) to determine the statistical differences among treatment sites (Biomass Removed and Biomass Left hillslopes), and treatment periods (pre- and post-harvest).

## Results and discussion

### Mercury tracer recovery and distribution

The enriched stable mercury isotope tracer was detected in subsurface runoff between May and August of each year (Fig. 2), while low concentrations of the $^{204}$Hg tracer (0.02–0.4 ng L$^{-1}$ at all hillslopes) were detected during the spring freshet in April 2013 (not shown). No mercury tracer was detected from the late summer through November in both years (Fig. 2). There was not a clear increase in ambient THg load post-harvest, nor was there an increase in average ambient THg concentrations (Fig. 2, Table 1). Runoff increased post-harvest, resulting in a greater total mass of mercury tracer in runoff at both harvested hillslopes (Table 1, Fig. 3). Post-harvest, there was an order of magnitude increase in the total mass of mercury tracer recovered at the harvested hillslopes (3.7–4.5 µg in 2011 and 30.0–54.0 µg in 2012), while the Unharvested Control hillslope was similar between years (11.8 µg in 2011 and 16.2 µg in 2012). In 2012, the 2011 tracer ($^{200}$Hg) accounted for, on average, 3, 5 and 1% of the mercury tracer at the Biomass Removed, Biomass Left and Unharvested Control hillslopes, respectively. Although there was a large increase in the total mass of tracer recovered in 2012, less than 2% of the total tracer applied to the surface was recovered at all sites for both years (Table 1). These low tracer recovery rates were within the observed recovery rates reported in other field and laboratory studies using isotopically enriched mercury isotopes in forests (Haynes and Mitchell 2015; Hintelmann et al. 2002; Oswald et al. 2014).

The low mercury tracer recovery in forests is often attributed to mercury retention in soils and the overall

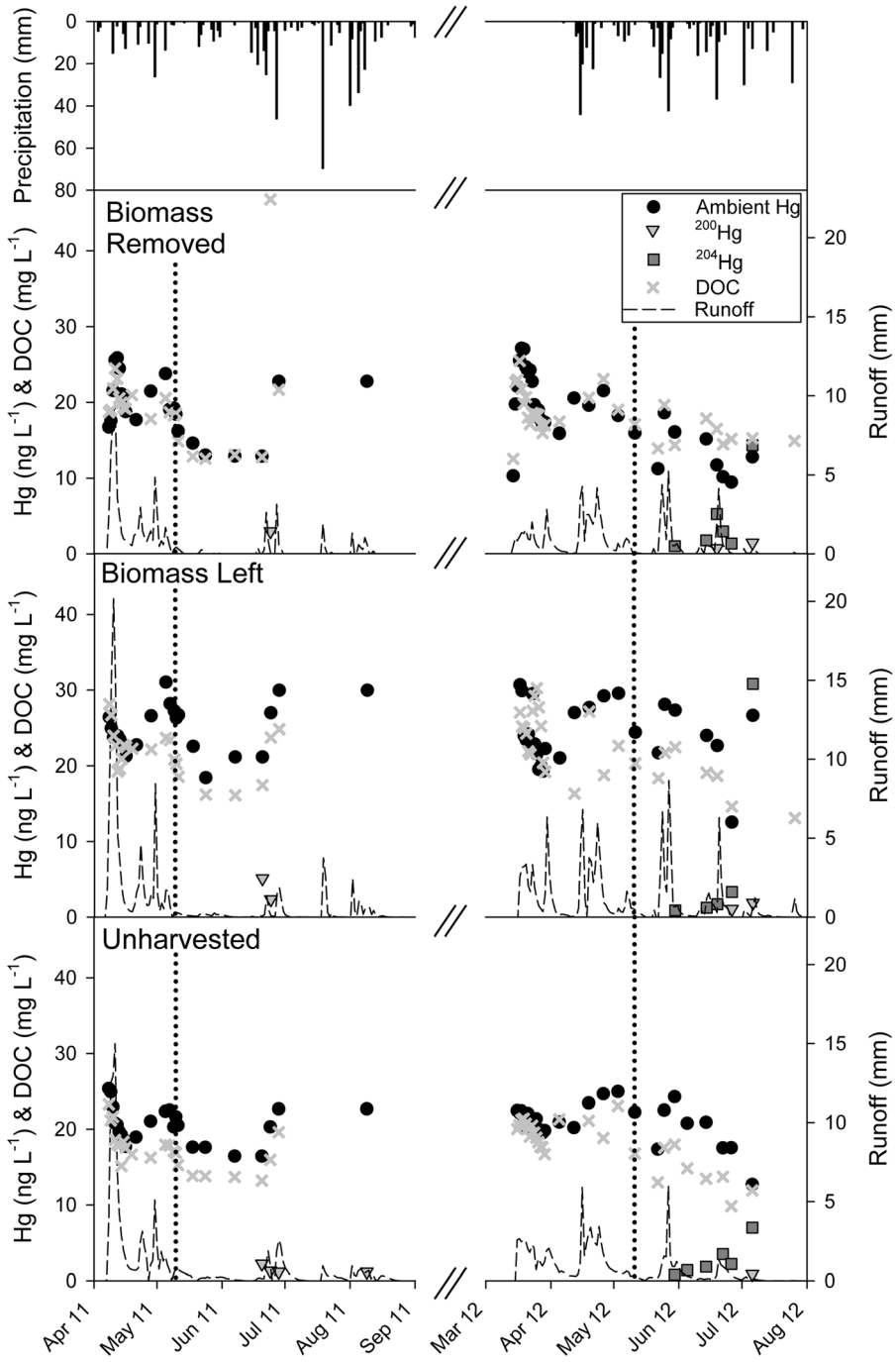


**Fig. 2** Ambient and tracer mercury concentrations and runoff at the Biomass Removed, Biomass Left and Unharvested Control hillslopes. Precipitation for both years is shown on the uppermost panel. The dashed vertical lines represent the application of tracer mercury. Runoff and precipitation data from McCarter et al. (2020a)

small total mass of tracer relative to the overall soil mercury pool (Haynes and Mitchell 2015; Hintelmann et al. 2002; Oswald et al. 2014). In this study, the total added mass of mercury tracer (0.007–0.009 g THg, 10.5 μg $m^{-2}$ $year^{-1}$) was several orders of magnitude less than the total ambient mercury soil pool

**Table 1** Average concentrations (± 1 standard deviation), mass loads and tracer recovery of ambient and tracer mercury from each experimental hillslope plot

| | | Biomass Left | Biomass Removed | Unharvested Control |
|---|---|---|---|---|
| 2011 (Pre-harvest) | | | | |
| Ambient THg | (ng $L^{-1}$) | 24.9 (3.2) | 19.3 (3.9) | 20.5 (2.5) |
| Tracer Hg | (ng $L^{-1}$) | 3.7 (2.0) | 3.0 (–) | 3.7 (2.0) |
| Ambient THg load | (µg) | 1144 | 764 | 1206 |
| Tracer Hg load | (µg) | 4.53 | 3.74 | 11.81 |
| Tracer recovery | – | 0.07% | 0.08% | 0.19% |
| Ratio to unharvested* | – | 0.38 | 0.32 | – |
| 2012 (Post-harvest) | | | | |
| Ambient THg | (ng $L^{-1}$) | 24.3 (4.2) | 18.5 (5.0) | 20.9 (2.5) |
| Tracer Hg | (ng $L^{-1}$) | 7.6 (13.0) | 4.5 (5.1) | 2.8 (2.3) |
| Ambient THg load | (µg) | 1206 | 759 | 1049 |
| Tracer Hg load | (µg) | 30.02 | 54.02 | 16.16 |
| Tracer recovery | – | 0.48% | 1.12% | 0.26% |
| Ratio to unharvested* | – | 1.86 | 3.34 | – |

(–) Indicates insufficient sample numbers to calculate a standard deviation

*Indicates the calculated ratio of the tracer recovery at a given treatment hillslope relative to the Unharvested Control hillslope for a given year

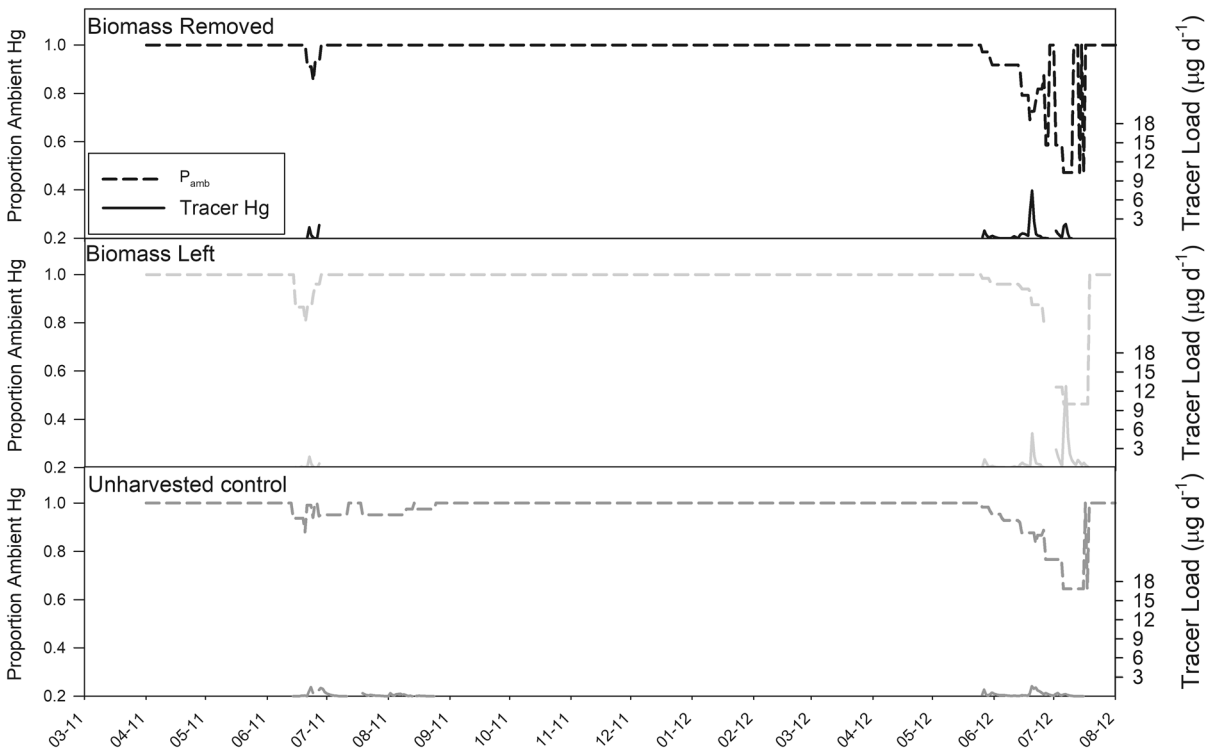


**Fig. 3** Timeseries of the proportion of ambient mercury ($P_{amb}$) in the subsurface runoff on the Biomass Removed (top), Biomass Left (middle) and Unharvested Control (bottom) hillslopes. Lower values indicate a greater proportion of tracer mercury mass recovered in relation to the total mercury mass. The dashed lines represent the application of tracer mercury

(1.7–2.3 g THg, 4.8–5.2 mg $m^{-2}$) determined by Haynes et al. (2017), resulting in an increase to the total sandy loam mercury pool by ~ 0.46% in 2011 and ~ 1.4% in 2012 due to the lower percent enrichment of the $^{204}$Hg tracer. Post-harvest (2012), Mazur et al. (2014) observed between 7 and 9% of the added mercury tracer was emitted to the atmosphere between May—November. At the Biomass Removed

and Unharvested Control hillslopes, about 50% of the applied $^{204}$Hg (2012 tracer) was entrained in the upper few centimeters of soil and litter and much less in the live vegetation and detrital layer (Mazur et al. 2014). Conversely, at the Biomass Left hillslope more than 50% of the $^{204}$Hg tracer was likely entrained within the detrital layer and live vegetation (unmeasured), with much less in the soils ($\sim$ 29%). Thus, $\sim$ 0.0009–0.005 g of the added mercury tracer was entrained within the soils, resulting in $<$ 1% of the soil entrained mercury being mobilized to the downgradient peatland. The rest of the mercury tracer will slowly leach out of the soils in minuscule quantities over time, likely well under our current detection limits.

## Forestry impacts on mercury pool mobilization

The enhanced mobilization of mercury post-harvest has been attributed to increased runoff from terrestrial landscapes (Eklöf et al. 2014; Porvari et al. 2003). If the overall runoff response governed the mercury response to harvesting, the change in mobilization to all mercury pools would likely systematically change with runoff. This pattern was not observed in this study. Pre-harvest (2011), ambient mercury was the dominant mercury (minimum 81–88% of THg) detected in subsurface runoff (Fig. 3). In contrast, post-harvest (2012) and at both harvested hillslopes, the proportion of ambient mercury at times significantly decreased ($p < 0.0001$) to $<$ 50% of the THg in subsurface runoff and the relative proportion of mercury tracer increased (Fig. 3). Although the proportion of mercury tracer significantly increased after harvesting, there were no significant differences in the proportion of ambient mercury between the two types of harvesting systems (Table S1). Similar to other enriched mercury isotope studies in forests (Oswald et al. 2014), few samples with detectable enriched mercury likely limited our ability to separate any differences between the two harvested hillslopes. Due to these low sample numbers, we were only able to detect the relatively large changes pre- and post-harvest, which is enabled by our use of two different enriched stable mercury isotope tracers.

The post-harvest response appears to be due to subtle changes in runoff generation pathways rather than, for example, changes in the pH of the precipitation, which could affect Hg mobility. Although changes in precipitation pH can drive enhanced mercury mobilization, chiefly through mobilization of DOC (Bishop et al. 2020), the precipitation pH (avg. 5.0) did not change during the study period from 2011 to 2012 at the nearby National Atmospheric Deposition Program site, MN16 [National Atmospheric Deposition Program (MN16) 2020], nor was any relationship between pH and DOC concentration observed during the study. Post-harvest, McCarter et al. (2020a) observed significant increases in runoff amount at both harvested sites over the frost-free seasons. The increased runoff was due to proportionally more near surface preferential flow relative to deeper subsurface flow such that more water from a given precipitation event would flow in the harvested plots through upper soil layers. A shift to shallow flowpaths would be expected to disproportionately increase mobilization of near-surface, recently deposited mercury tracer. Jiskra et al. (2017) observed a non-significant, but twofold, increase in the contribution of mercury from Oa/Ha horizons in stream runoff from a boreal forest harvested site in Sweden using natural abundance mercury isotopes and chemical fingerprinting techniques. In this study, we observed a disproportionate increase in recently deposited near-surface mercury mobilized due to changes in the proportioning of water to near surface flow pathways post-harvest, regardless of harvesting type. These near-surface flow paths were likely constrained to the upper few centimeters of soil given that a large proportion of the mercury tracer was observed to be entrained in the upper 2 cm (Mazur et al. 2014). Therefore, forest management may not only impact the overall mobilization of mercury, but also whether more recently added or legacy pools of mercury are predominantly mobilized to downgradient ecosystems.

There were overarching controls on mobilization of the different mercury pools that go beyond forest harvesting practices, as indicated by: (1) the lack of statistical difference between the two harvesting treatments (Fig. S1) and (2) the similarity of the mercury concentrations (Fig. 2) and proportion of ambient mercury (Fig. 3) among all three hillslopes within a given year. Though different harvesting practices do not appear to strongly affect recently deposited mercury mobilization, the breadth of hydrological and biogeochemical conditions observed in this study allow for further correlative analyses of hydroclimatic and chemical metrics to infer possible

mechanisms governing the mobilization of mercury on hillslopes.

## Mercury and dissolved organic carbon

In many ecosystems, DOM is thought to be the dominant ligand associated with the mobilization of mercury (Bishop et al. 2020), where positive, often linear, relationships between DOC and mercury concentrations are common (Åkerblom et al. 2008; Driscoll et al. 1995; Kolka et al. 1999; Riscassi and Scanlon 2011; Skyllberg et al. 2009). At all hillslopes in this study, ambient THg concentrations in hillslope runoff significantly ($p < 0.001$) and positively correlated to DOC concentrations across all study years (2010–2013), regardless of harvest type. However, the relationships deviated from linearity at low DOC concentrations (Fig. 4, Table S2). Though a broadly significant DOC-ambient THg relationship was maintained across the three hillslopes (Fig. S2, Table S2), the slopes at each hillslope increased, though not significantly so, from unharvested control < biomass left < biomass removed (Fig. 4). The broader significant relationship suggests that there is a hillslope independent DOC-ambient THg relationship that was impacted by local characteristics, such as differences in soil organic matter content, soil thickness, or soil water residence time on each hillslope.

In contrast to ambient mercury, there were negative or insignificant relationships between mercury tracer and DOC concentrations in runoff, regardless of hillslope or harvest type (Fig. 4, Table S2). Additionally, the average DOC concentrations for a given runoff event across all hillslopes were not correlated with the average mercury tracer concentration for a runoff event (Fig. 5a). Haynes and Mitchell (2015) previously observed significant linear relationships between both tracer and ambient mercury and DOC in a soil monolith experiment from the same hillslope, but these relationships occurred when mercury concentrations were well above those observed in this study (< 50 ng $L^{-1}$). We speculate that the complexation of mercury tracer to DOM was rate limited within the upper soil layer due to a predominance of near surface flow. Unlike the steady-state flow and water level conditions of the Haynes and Mitchell (2015) study, we observed periods of disproportionally high runoff with minimal saturation above the clay loam till (McCarter et al. 2020a). Though we

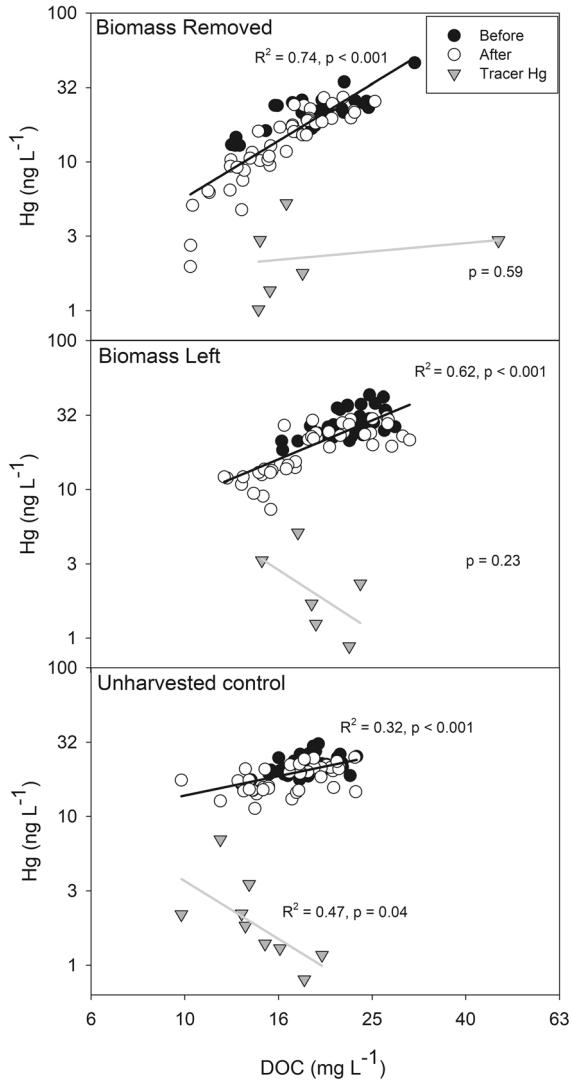


**Fig. 4** The relationship between DOC and both ambient and tracer mercury concentrations in runoff from the Biomass Removed (top), Biomass Left (middle) and Unharvested Control (bottom) hillslopes. The ambient mercury relationships were determined from the lumped pre- and post-harvest data from 2010 to 2013 and are separated for visual clarity. All axes are on a $\log_{10}$ scale and the resultant functions fit a 2-variable power function on linear scales

consistently observed MeHg concentrations below detection limits (< 0.02 ng $L^{-1}$) in runoff from the hillslopes and eventually ceased sample analysis for MeHg, negative relationships between DOC and MeHg have been previously observed due to rate limitation of MeHg production during high flow events (e.g. Bishop and Lee 1997). Relative to rate constants for methylation (Tjerngren et al. 2012), the

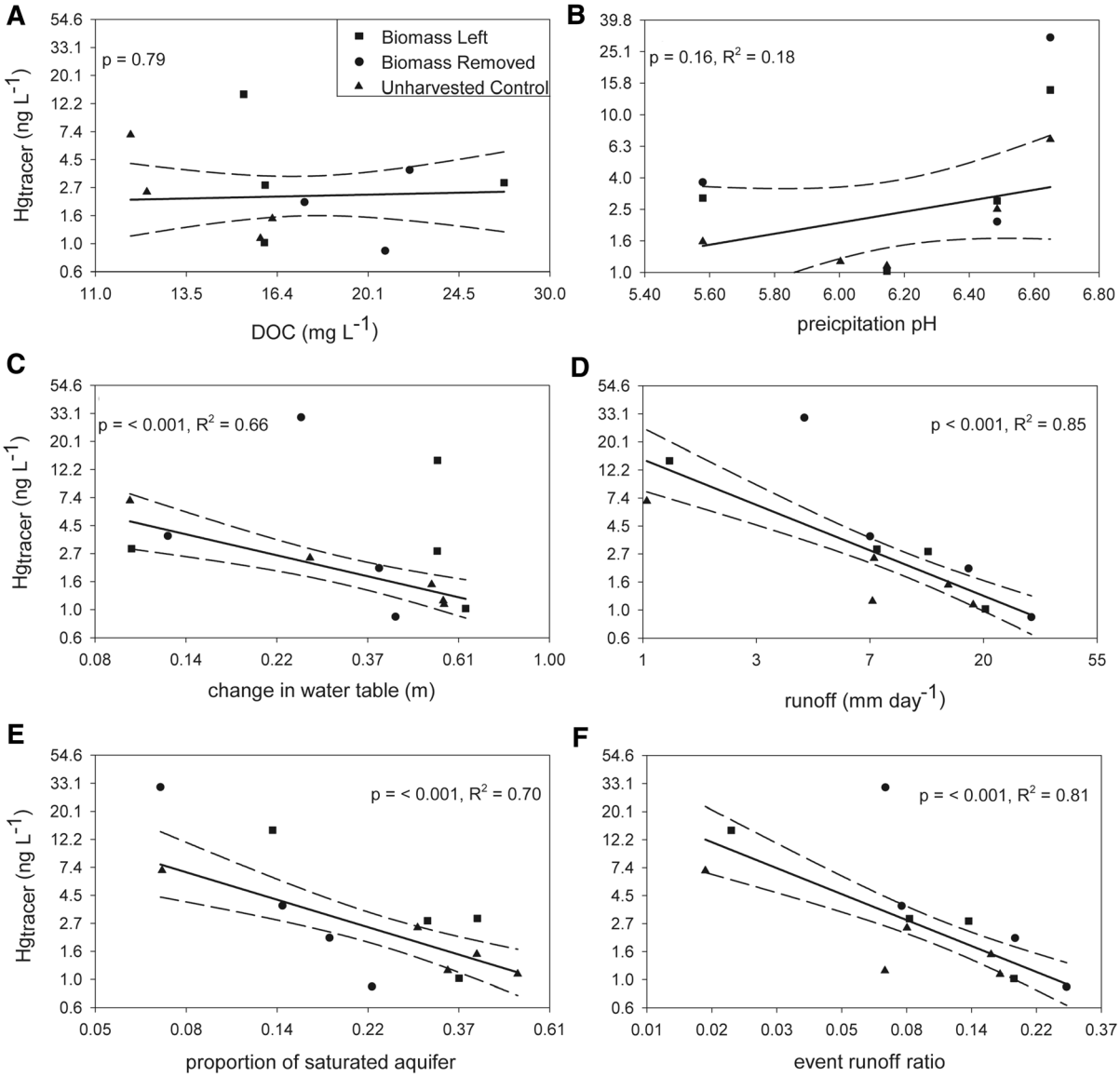


**Fig. 5** Bivariate regressions between average event tracer mercury concentrations and **A** event DOC concentration, **B** event precipitation pH, **C** change in water table from the start of an event to the peak event water table, **D** event runoff, **E** the proportion of the sandy loam aquifer that is saturated (low values indicate a water table near the low-permeability Koochiching clay loam till), and **F** event runoff ratio. The dashed lines are the 95% confidence intervals of the regression. All axes are on a $\log_e$ scale, except for panel **B**. The resultant functions fit a 2-variable power function on linear scales

rate constants for the complexation of inorganic mercury, Hg(II), to DOM are much higher, often achieving equilibrium within hours (Miller et al. 2009). When high flow velocities and short hydrological residence times occurred with near surface saturation and shallow subsurface flow, mercury tracer was potentially removed from the solid phase by rapid equilibrium exchange with the aqueous phase (Blanc et al. 2018; Hintelmann et al. 1997; Leterme et al. 2014; Miller et al. 2009). Subsequent complexation to mobile DOM could be rate-limited due to the short hydrological residence times, as observed with the mobilization of other metals (Jacques et al. 2008), or low mercury tracer concentrations (Leterme et al. 2014). Alternatively, the DOC concentration in the pore water of the upper few cm of soil could be high

with respect to the mercury tracer concentration and an increase in DOC concentration does not necessarily correspond to a change in the mercury tracer concentration, as observed in a nearby peatland-fed stream with high DOC concentrations (Woerndle et al. 2018). Together, these results highlight that DOM-Hg(II) interactions may play a more minor role in recently deposited Hg(II) mobilization in situations where hillslope hydrological flowpaths are shallow and residence times are relatively short.

## Drivers of mercury mobilization

Runoff events and the subsequent subsurface stormflow are drivers of ambient mercury mobilization on the hillslopes at MEF (Woerndle et al. 2018). The different observed mobilization and Hg-DOC relationships of the ambient and mercury tracer pools were potentially driven by the prevalence of preferential subsurface flow during runoff events at this hillslope for several clear time periods (Table 2). Preferential subsurface flow on hillslopes can be generated by both direct lateral flow through interconnected macropores (Buttle and McDonald 2002; Kim et al. 2004, 2005; Tsuboyama et al. 1994; Weiler and McDonnell 2004, 2007) and vertical macropore flow, where water and solutes are rapidly transmitted downward to the impermeable layer (in this case the Koochiching clay loam till) and then move downhill above an aquitard (Beven and Germann 1982; Buttle and McDonald 2002; Freer et al. 2002; Germann and Beven 1986; McDonnell 1990; Noguchi et al. 2001). For the latter to occur, the soils directly above the impermeable layer would need to be unsaturated through much of the profile prior to the precipitation events. There was a moderate negative relationship between the antecedent soil moisture 5 cm above the sandy loam-clay loam interface and event mercury tracer load (Fig. S3), and no relationship with average mercury tracer concentration. However, this analysis was limited by the failure of the soil moisture probes at the Unharvested Control hillslope and that the soil moisture measurement point was nearer the mid-slope rather than nearer the runoff trench, which likely represents different hydrological conditions due to the observed downslope hydraulic gradients (McCarter et al. 2020a). No significant correlations between mercury tracer load for a given runoff event and hydrological metrics (runoff amount, runoff ratio, change in water table, and proportion of saturated aquifer) were observed, while ambient mercury loads did correlate to runoff amounts, as expected from Eq. 1. However, the highest mercury tracer concentrations occurred when the change in hydraulic gradient from the top to toe of the hillslope was closest to zero, suggesting limited hydrological connectivity from the top to toe of slope (Table 2). On these hillslopes, it appears that distinct hydrological processes drove the mobilization of the different mercury pools, where ambient mercury was mobilized under saturated flow conditions and the more recently deposited mercury under more preferential flow conditions.

Average mercury tracer concentration for a runoff event did not correlate with average event DOC concentration (Fig. 5a) or with the average weekly precipitation pH (Fig. 5b). Rather, average mercury tracer concentration for a runoff event negatively correlated with hydrological connectivity metrics, such as runoff amount and runoff ratio (Fig. 5d, f), and with water table metrics (Fig. 5c, e). Despite the increase in mercury tracer during small precipitation events, the majority of mercury mobilized from the hillslopes was from the ambient mercury pool and recently (*i.e.*, within a few weeks) deposited mercury mobilization was low. As the water table decreased in the sandy loam aquifer, towards the low-permeability clay loam till, the effective hydraulic conductivity decreased exponentially on these hillslopes (McCarter et al. 2020a). The exponential decline in hydraulic conductivity would limit the effective downward movement of precipitation, particularly during small precipitation events. These small precipitation events (Fig. S4) led to a muted runoff generation and water table response, and low event runoff ratios (Fig. 5e, f). The runoff amount for a given precipitation event decreased when the precipitation amount was lower and precipitation was less frequent, corresponding to the proportion of mercury tracer increasing in the runoff (Fig. 5d, f). These conditions typically occurred during late June through August and coincided with the lowest $P_{amb}$ values, highest mercury tracer loads (Fig. 3), low effective hydraulic conductivity, and smallest change in hillslope hydraulic gradient (Table 2), suggesting a disconnect of the surficial mercury tracer from deeper soils and saturated flow. In 2012, Mazur et al. (2014) observed between 1.5 and 5 μg $^{204}$Hg m$^{-2}$ of the 10.5 μg $^{204}$Hg m$^{-2}$ mercury tracer within the upper 2 cm of soil. The

**Table 2** Hydrological parameters and chemical loads resulting from precipitation events after the mercury tracer application in both 2011 and 2012

| | Event start | Precipitation end | Runoff end | Precipitation (mm) | Runoff (mm) | Runoff ratio – | Max water table (m asl) | Antecedent water table (m asl) | Change in water table (m) | Change in hydraulic gradient* – | Effective hydraulic conductivity (m $day^{-1}$) | Mercury tracer conc (ng $L^{-1}$) | Ambient mercury conc (ng $L^{-1}$) |
|---|---|---|---|---|---|---|---|---|---|---|---|---|---|
| Biomass Removed | June 20, 2011 | June 30, 2011 | July 10, 2011 | 23 | 8 | 0.34 | 433.27 | 433.17 | 0.10 | 3.1E-03 | 0.12 | 3.0 | 5.9 |
| | July 18, 2011 | July 31, 2011 | July 31, 2011 | 10 | 2 | 0.24 | 433.15 | 432.62 | 0.53 | 6.4E-06 | 0.25 | – | 6.0 |
| | August 1, 2011 | August 13, 2011 | August 23, 2011 | 13 | 5 | 0.35 | 433.22 | 432.77 | 0.44 | 2.4E-03 | 0.11 | – | 5.0 |
| | May 20, 2012 | June 5, 2012 | June 7, 2012 | 101 | 20 | 0.20 | 433.27 | 432.64 | 0.63 | − 2.1E-03 | 0.23 | 1.0 | 8.2 |
| | June 8, 2012 | June 25, 2012 | June 30, 2012 | 86 | 12 | 0.14 | 433.27 | 432.73 | 0.54 | 1.2E-03 | 0.13 | 2.8 | 3.1 |
| | July 1, 2012 | July 15, 2012 | July 24, 2012 | 44 | 1 | 0.03 | 433.17 | 432.63 | 0.54 | − 3.3E-05 | 0.06 | 14.4 | 0.7 |
| Biomass Left | June 20, 2011 | June 30, 2011 | July 10, 2011 | 23 | 7 | 0.32 | 431.44 | 431.32 | 0.12 | − 1.5E-03 | 0.14 | 3.7 | 3.8 |
| | July 18, 2011 | July 31, 2011 | July 31, 2011 | 10 | 7 | 0.71 | 431.35 | 431.11 | 0.24 | − 1.8E-05 | 0.91 | – | 6.0 |
| | August 1, 2011 | August 13, 2011 | August 23, 2011 | 13 | 8 | 0.60 | 431.37 | 431.11 | 0.26 | 3.0E-05 | 0.16 | – | 3.6 |
| | May 20, 2012 | June 5, 2012 | June 7, 2012 | 101 | 31 | 0.30 | 431.55 | 431.12 | 0.43 | − 1.6E-04 | 2.13 | 0.9 | 16.3 |
| | June 8, 2012 | June 25, 2012 | June 30, 2012 | 86 | 18 | 0.21 | 431.51 | 431.12 | 0.39 | − 1.4E-05 | 0.68 | 2.1 | 6.3 |
| | July 1, 2012 | July 15, 2012 | July 24, 2012 | 44 | 4 | 0.10 | 431.37 | 431.12 | 0.26 | 2.4E-05 | 0.07 | 30.8 | 1.6 |
| Unharvested Control | June 20, 2011 | June 30, 2011 | July 10, 2011 | 23 | 15 | 0.65 | 430.00 | 429.48 | 0.52 | − 6.8E-04 | 0.12 | 1.6 | 8.2 |
| | July 18, 2011 | July 31, 2011 | July 31, 2011 | 10 | 4 | 0.39 | 429.67 | 429.25 | 0.41 | 3.8E-04 | 0.11 | – | 3.2 |
| | August 1, 2011 | August 13, 2011 | August 23, 2011 | 13 | 8 | 0.59 | 429.97 | 429.41 | 0.56 | 1.2E-03 | 0.08 | 1.2 | 3.6 |
| | May 20, 2012 | June 5, 2012 | June 7, 2012 | 101 | 18 | 0.18 | 430.12 | 429.56 | 0.56 | − 9.5E-04 | 0.13 | 1.1 | 10.1 |
| | June 8, 2012 | June 25, 2012 | June 30, 2012 | 86 | 8 | 0.09 | 429.81 | 429.55 | 0.27 | 1.7E-03 | 0.07 | 2.5 | 2.8 |
| | July 1, 2012 | July 15, 2012 | July 24, 2012 | 44 | 1 | 0.02 | 429.48 | 429.38 | 0.10 | 1.7E-03 | 0.04 | 7.0 | 0.4 |

(–) Indicates no measured concentration

*Indicates the change in hydraulic gradient from the top to toe of slope from the antecedent water table to the maximum water table

disconnect between the surficial mercury tracer and deeper saturated flow was likely driven by rainwater that mobilized the mercury tracer from surficial soil layers nearer the runoff trenches. We speculate that the runoff events associated with higher mercury tracer concentrations likely resulted from some form of rapid mobilization and preferential flow with little change in the overall hillslope hydrology (as evidenced by changes in hillslope hydraulic gradients close to 0 and low effective hydraulic conductivity), rather than transport from a thick saturated layer as observed with the ambient mercury. However, this rapid and preferential routing remains an open question in terrestrial mercury research. Despite our lack of clarity on the mechanism, the mobilization of the different mercury pools (recent tracer or ambient) had an important dependency on routing of precipitation to different subsurface flow paths.

The variation and elevation of the water table has been shown to strongly govern the mobilization of mercury tracer in previous studies (Branfireun et al. 2005; Oswald et al. 2014). Branfireun et al. (2005) observed an increase in mercury tracer concentrations with increasing water table in a boreal wetland, while Oswald et al. (2014) found that preferential flow paths in well drained boreal forest hillslopes accelerated the movement of the applied mercury tracer to topographic lows, similar to this study. Furthermore, Oswald et al. (2014) observed that the downward vertical transport of mercury tracer through the organic horizon to deep soils was an important flowpath. This downward transport was primarily driven by the rise in water table to within the organic horizon, which mobilized a disproportionate mass of mercury tracer that was entrained in these soils. The subsequent decline of the water table to the deeper mineral soils would facilitate the downward transport of the mercury tracer (Oswald et al. 2014). Here, the shallow soils and intermittent water table on these hillslopes limited the water table dependent downward transport of the mercury tracer due to less water table fluctuation within the near-surface organic layer (McCarter et al. 2020a) that contained a majority of mercury tracer within the soil. This limited movement of mercury tracer to the runoff collector was associated with larger saturated thicknesses of the sandy loam aquifer (Fig. 4e). Essentially, the mobilization of the recently deposited mercury was disconnected from the bulk water flow that was observed in other field-scale enriched mercury tracer studies (Branfireun et al. 2005; Oswald et al. 2014). These results illustrate the importance of understanding the variability in the hydrological setting in accurately characterizing the movement of mercury across a landscape.

## Implications for mercury dynamics

Mercury can enter soils through both wet and dry deposition (Bishop et al. 2020). Wet deposition is driven by precipitation through Hg(II) within water droplets in clouds or as particulate-bound Hg(II) (Landis et al. 2002), while dry deposition occurs when elemental $Hg^0$ is incorporated into the organic structure of growing vegetation and falls to the ground during senescence (Bishop et al. 2020; Demers et al. 2007). Of these two primary mechanisms, dry deposition makes up the majority of mercury inputs into the terrestrial environment from the atmosphere (Bishop et al. 2020; Demers et al. 2013; Zhou et al. 2021). However, once in the terrestrial environment the initial mobility of these two inputs is often different. Dry deposition is often incorporated into organic matter (*e.g.*, leaves or woody debris) and is likely much less mobile, at least until additional decomposition processes or surface erosion occur (Demers et al. 2007; Pokharel and Obrist 2011). Conversely, with wet deposition, Hg(II) does not necessarily require additional time-intensive processes like the decomposition of solid organic matter to become part of the more hydrologically mobile pool in terrestrial systems (Bishop et al. 2020). The application of dissolved Hg(II) tracers in this study represents the transport pathways that govern mercury movement in the terrestrial environment either directly from wet deposition or after decomposition processes have liberated dry deposited mercury bound in soil organic matter. The latter can offset the input of atmospheric mercury by years to decades due to decomposition processes that depend on specific soil, litter and environmental conditions (Hall and St. Louis 2004; Pokharel and Obrist 2011). Under constant dry deposition and subsequent decomposition rates, the overall mobility of mercury, thus flux of mercury, in terrestrial environments will be primarily dependent on the mercury mobilization processes explored in this study.

It is uncertain how long any reduction in atmospheric mercury deposition will take to produce clearly decreased mercury concentrations in surface

water and groundwater (Hintelmann et al. 2002; Osterwalder et al. 2017). In previous research, Harris et al. (2007) suggested that watersheds with larger terrestrial upland areas contributing runoff to lakes would have substantially longer recovery compared to lakes with smaller terrestrial watersheds. Our work refines that perspective by more closely examining how the hydrology of upland systems might impact this timing, particularly in relation to overlapping influences, such as global climate change. Climate change will alter the timing and magnitude of precipitation events and antecedent hydrological conditions (IPCC 2014), which are likely to alter the mobilization of mercury from terrestrial landscapes (Haynes et al. 2017; Pompeani et al. 2018). These results lead us to suggest that mercury mobilization under both undisturbed and disturbed (*e.g.*, forest harvesting) conditions differs for legacy stores of soil mercury versus more recently deposited mercury and that the depth below the surface and flowpath routing on a given hillslope are primary controls on how much recently deposited and legacy mercury are mobilized. A shift to a climate that increases the relative proportion of near surface flow (*i.e.*, more sporadic small precipitation events) would increase the mobility of more recently deposited atmospheric mercury pools (*e.g.*, deposited within one year) in systems such as this study area. However, under a future climate with more frequent and larger precipitation events, also predicted for the study region (Hayhoe et al. 2010; Pryor and Scavia 2014), it is likely that a greater proportion of mercury will be mobilized from deeper flow paths, representing a larger proportion of the older ambient mercury. This increase in older ambient mercury may be, at least partially, offset by increases in evapotranspiration and longer periods without precipitation (Dymond et al. 2014; Pryor and Scavia 2014), lowering near-surface soil moisture and increasing the near-surface preferential mobilization of recently deposited mercury from hillslopes during shorter and more intense precipitation events. Cumulatively, the proportion of recently deposited mercury vs. legacy mercury in runoff will affect how quickly reductions in atmospheric deposition may translate to reductions in mercury contamination of downstream aquatic systems.

## Conclusions

Although preferential mobilization of near-surface recently deposited mercury occurred, recently deposited mercury tracer was a small fraction of the mercury mobilized from hillslopes. The amount of recently deposited mercury tracer observed in runoff was unrelated to either DOC concentrations or precipitation pH, but was strongly, negatively correlated with hydrological factors such as event runoff volumes and runoff ratios. The direction of these relationships suggests that a greater proportion of more recently deposited mercury is preferentially mobilized downslope occurs during low precipitation and low runoff events. No significant differences in the mobilization of recently deposited mercury were observed whether or not residual biomass was harvested. This finding may be due to low sample numbers that are common in field-scale enriched stable mercury isotope tracer studies. Despite the lack of difference between harvesting treatments, harvesting, in general, clearly and significantly increased the proportion of recently deposited mercury in runoff due to changes in the hillslope hydrology. The different precipitation, runoff amounts, and antecedent conditions between the study years and hillslopes suggests that climate may exert a stronger control on the mobilization of different mercury pools. Therefore, changes in the timing and magnitude of precipitation events under climate change may alter how quickly reductions in atmospheric mercury concentrations translate into lower mercury concentrations in aquatic ecosystems that are hydrologically connected to low-topographic relief forests.

**Acknowledgements** We wish to thank the staff at the Marcell Experimental Forest Research Station for logistical support. In particular we thank Deacon Kyllander, Carrie Dorrance, Nate Aspelin, Josh Kragthorpe, Reid Peterson, Leigh Kastenson, Madeline Wiley, Mitchell Olds, Ben Munson, Paul Watson, Ross Bentson, Mike Palmer, Doris Nelson, Nicole King, Gerrard Graves, Donna Olson, and Anne Timm of the Northern Research Station (USDA Forest Service), and Jeromie Geroatte and Stephen Stalheim of the US Job Corps for their assistance with field work. Maxwell Mazur, Kristine Haynes and Haiyong (Planck) Huang provided important field and laboratory support. We thank Dwight Streblow, who harvested the plots in 2012. We would also like to thank three anonymous reviewers whose comments and suggestions improved the manuscript.

**Funding** We acknowledge the support of funding from the Great Lakes Air Deposition Program (GLAD 2010-7) and the Natural Sciences and Engineering Research Council of Canada (Funding Reference Number 355866-18) to CPJM as well as a Natural Sciences and Engineering Research Council of Canada Postdoctoral Fellowship to CPRM. The Northern Research Station of the USDA Forest Service paid for forest harvesting, and funded the salaries of SDS, RKK, and SLE.

**Data Availability** The datasets generated during and/or analysed during the current study are available in the U.S. Forest Service Research Data Archive, as McCarter et al. (2020b) https://doi.org/10.2737/RDS-2020-0049 and McCarter et al. (2021) https://doi.org/10.2737/RDS-2021-0007.

**Declarations**

**Conflict of interest** The authors have no conflict of interest to declare that are relevant to the content of this article.

## References

Åkerblom S, Meili M, Bringmark L, Johansson K, Kleja DB, Bergkvist B (2008) Partitioning of Hg between solid and dissolved organic matter in the humus layer of boreal forests. Water Air Soil Poll 189:239–252. https://doi.org/10.1007/s11270-007-9571-1

APHA (2017) Standard methods for the examination of water and wastewater, 23rd edn. American Public Health Association, Washington, DC

Beven K, Germann P (1982) Macropores and water flow in soils. Water Resour Res 18:1311–1325. https://doi.org/10.1029/WR018i005p01311

Bishop KH, Lee YH (1997) Catchments as a source of mercury/methylmercury in boreal surface waters. In: Sigel A, Sigel H (eds) Metal ions in biological systems: mercury and its effect on environment and biology, vol 34. Hindawi Publishing Corporation, Nanjing, pp 113–130. https://doi.org/10.1155/MBD.1997.287

Bishop K et al (2009) The effects of forestry on Hg bioaccumulation in nemoral/boreal waters and recommendations for good silvicultural practice. Ambio 38:373–380. https://doi.org/10.1579/0044-7447-38.7.373

Bishop K et al (2020) Recent advances in understanding and measurement of mercury in the environment: terrestrial Hg cycling. Sci Total Environ 721:137647. https://doi.org/10.1016/j.scitotenv.2020.137647

Blanc P, Burnol A, Marty N, Hellal J, Guérin V, Laperche V (2018) Methylmercury complexes: selection of thermodynamic properties and application to the modelling of a column experiment. Sci Total Environ 621:368–375. https://doi.org/10.1016/j.scitotenv.2017.11.259

Branfireun BA, Krabbenhoft DP, Hintelmann H, Hunt RJ, Hurley JP, Rudd JWM (2005) Speciation and transport of newly deposited mercury in a boreal forest wetland: a stable mercury isotope approach. Water Resour Res 41:W06016. https://doi.org/10.1029/2004wr003219

Buttle JM, McDonald DJ (2002) Coupled vertical and lateral preferential flow on a forested slope. Water Resour Res. 38:18–11–18–16. https://doi.org/10.1029/2001WR000773

Conner MM, Saunders WC, Bouwes N, Jordan C (2016) Evaluating impacts using a BACI design, ratios, and a Bayesian approach with a focus on restoration. Environ Monit Assess 188:555. https://doi.org/10.1007/s10661-016-5526-6

Demers JD, Driscoll CT, Fahey TJ, Yavitt JB (2007) Mercury cycling in litter and soil in different forest types in the Adirondack region, New York, USA. Ecol Appl 17:1341–1351. https://doi.org/10.1890/06-1697.1

Demers JD, Blum JD, Zak DR (2013) Mercury isotopes in a forested ecosystem: implications for air-surface exchange dynamics and the global mercury cycle. Global Biogeochem Cycles 27:222–238. https://doi.org/10.1002/gbc.20021

Devito KJ, Creed IF, Rothwell RL, Prepas EE (2000) Landscape controls on phosphorus loading to boreal lakes: implications for the potential impacts of forest harvesting. Can J Fish Aquat Sci 57:1977–1984. https://doi.org/10.1139/f00-148

Driscoll CT, Blette V, Yan C, Schofield CL, Munson R, Holsapple J (1995) The role of dissolved organic carbon in the chemistry and bioavailability of mercury in remote Adirondack lakes. Water Air Soil Poll 80:499–508. https://doi.org/10.1007/bf01189700

Dymond SF, Kolka RK, Bolstad PV, Sebestyen SD (2014) Long-term soil moisture patterns in a northern Minnesota forest. Soil Sci Soc Am J 78:S208–S216. https://doi.org/10.2136/sssaj2013.08.0322nafsc

Eklöf K, Schelker J, Sørensen R, Meili M, Laudon H, von Brömssen C, Bishop K (2014) Impact of forestry on total and methyl-mercury in surface waters: distinguishing effects of logging and site preparation. Environ Sci Technol 48:4690–4698. https://doi.org/10.1021/es404879p

Eklöf K, Lidskog R, Bishop K (2016) Managing Swedish forestry's impact on mercury in fish: defining the impact and mitigation measures. Ambio 45:163–174. https://doi.org/10.1007/s13280-015-0752-7

Eklöf K et al (2018) Formation of mercury methylation hotspots as a consequence of forestry operations. Sci Total Environ 613–614:1069–1078. https://doi.org/10.1016/j.scitotenv.2017.09.151

Ericksen JA, Gustin MS, Lindberg SE, Olund SD, Krabbenhoft DP (2005) Assessing the potential for re-emission of mercury deposited in precipitation from arid soils using a stable isotope. Environ Sci Technol 39:8001–8007. https://doi.org/10.1021/es0505651

Freer J et al (2002) The role of bedrock topography on subsurface storm flow. Water Resour Res 38:5–1–5–16. https://doi.org/10.1029/2001WR000872

Gai K, Hoelen TP, Hsu-Kim H, Lowry GV (2016) Mobility of four common mercury species in model and natural unsaturated soils. Environ Sci Technol 50:3342–3351. https://doi.org/10.1021/acs.est.5b04247

Germann PF, Beven K (1986) A distribution function approach to water flow in soil macropores based on kinematic wave theory. J Hydrol 83:173–183. https://doi.org/10.1016/0022-1694(86)90191-5

Hale CM, Frelich LE, Reich PB (2005) Exotic European earthworm invasion dynamics in northern hardwood forests of Minnesota, USA. Ecol Appl 15:848–860. https://doi.org/10.1890/03-5345

Hall BD, St. Louis VL (2004) Methylmercury and total mercury in plant litter decomposing in upland forests and flooded landscapes. Environ Sci Technol 38:5010–5021. https://doi.org/10.1021/es049800q

Harris RC et al (2007) Whole-ecosystem study shows rapid fish-mercury response to changes in mercury deposition. Proc Natl Acad Sci USA 104:16586–16591. https://doi.org/10.1073/pnas.0704186104

Hayhoe K, VanDorn J, Croley T, Schlegal N, Wuebbles D (2010) Regional climate change projections for Chicago and the US Great Lakes. J Great Lakes Res 36:7–21. https://doi.org/10.1016/j.jglr.2010.03.012

Haynes KM, Mitchell CPJ (2012) Inter-annual and spatial variability in hillslope runoff and mercury flux during spring snowmelt. J Environ Monit 14:2083–2091. https://doi.org/10.1039/C2EM30267E

Haynes KM, Mitchell CPJ (2015) Precipitation input and antecedent soil moisture effects on mercury mobility in soil—laboratory experiments with an enriched stable isotope tracer. Hydrol Process 29:4161–4174. https://doi.org/10.1002/hyp.10442

Haynes KM, Kane ES, Potvin L, Lilleskov EA, Kolka RK, Mitchell CPJ (2017) Mobility and transport of mercury and methylmercury in peat as a function of changes in water table regime and plant functional groups. Global Biogeochem Cycles 31:233–244. https://doi.org/10.1002/2016GB005471

Hintelmann H, Ogrinc N (2002) Determination of stable mercury isotopes by ICP/MS and their application in environmental studies. In: Biogeochemistry of environmentally important trace elements, vol 835. ACS Symposium Series, vol 835. American Chemical Society, pp 321–338. http://doi.org/https://doi.org/10.1021/bk-2003-0835.ch021

Hintelmann H, Welbourn PM, Evans RD (1997) Measurement of complexation of methylmercury(ii) compounds by freshwater humic substances using equilibrium dialysis. Environ Sci Technol 31:489–495. https://doi.org/10.1021/es960318k

Hintelmann H et al (2002) Reactivity and mobility of new and old mercury deposition in a boreal forest ecosystem during the first year of the METAALICUS study. Environ Sci Technol 36:5034–5040. https://doi.org/10.1021/es025572t

Holub SM, Terry TA, Harrington CA, Harrison RB, Meade R (2013) Tree growth ten years after residual biomass removal, soil compaction, tillage, and competing vegetation control in a highly-productive Douglas-fir plantation. For Ecol Manag 305:60–66. https://doi.org/10.1016/j.foreco.2013.05.031

Hsu-Kim H, Eckley CS, Achá D, Feng X, Gilmour CC, Jonsson S, Mitchell CPJ (2018) Challenges and opportunities for managing aquatic mercury pollution in altered landscapes. Ambio 47:141–169. https://doi.org/10.1007/s13280-017-1006-7

IPCC (2014) Climate change 2014: synthesis report. Contribution of working groups i, ii and iii to the fifth assessment report of the intergovernmental panel on climate change. IPCC, Geneva

Jacques D, Šimůnek J, Mallants D, van Genuchten MT (2008) Modelling coupled water flow, solute transport and geochemical reactions affecting heavy metal migration in a podzol soil. Geoderma 145:449–461. https://doi.org/10.1016/j.geoderma.2008.01.009

Janowiak MK, Webster CR (2010) Promoting ecological sustainability in woody biomass harvesting. J For 108:16–23. https://doi.org/10.1093/jof/108.1.16

Jiskra M, Wiederhold JG, Skyllberg U, Kronberg R-M, Kretzschmar R (2017) Source tracing of natural organic matter bound mercury in boreal forest runoff with mercury stable isotopes. Environ Sci-Proc Imp 19:1235–1248. https://doi.org/10.1039/C7EM00245A

Kim HJ, Sidle RC, Moore RD, Hudson R (2004) Throughflow variability during snowmelt in a forested mountain catchment, coastal British Columbia, Canada. Hydrol Process 18:1219–1236. https://doi.org/10.1002/hyp.1396

Kim HJ, Sidle RC, Moore RD (2005) Shallow lateral flow from a forested hillslope: influence of antecedent wetness. CATENA 60:293–306. https://doi.org/10.1016/j.catena.2004.12.005

Kolka RK, Grigal DF, Verry ES, Nater EA (1999) Mercury and organic carbon relationships in streams draining forested upland/peatland watersheds. J Environ Qual 28:766–775. https://doi.org/10.2134/jeq1999.00472425002800030006x

Kolka RK, Grigal DF, Nater EA, Verry ES (2001) Hydrologic cycling of mercury and organic carbon in a forested upland–bog watershed. Soil Sci Soc Am J 65:897–905. https://doi.org/10.2136/sssaj2001.653897x

Kreutzweiser DP, Hazlett PW, Gunn JM (2008) Logging impacts on the biogeochemistry of boreal forest soils and nutrient export to aquatic systems: a review. Environ Rev 16:157–179. https://doi.org/10.1139/A08-006

Kronberg R-M, Drott A, Jiskra M, Wiederhold JG, Björn E, Skyllberg U (2016) Forest harvest contribution to boreal freshwater methyl mercury load. Global Biogeochem Cycles 30:825–843. https://doi.org/10.1002/2015gb005316

Landis MS, Stevens RK, Schaedlich F, Prestbo EM (2002) Development and characterization of an annular denuder methodology for the measurement of divalent inorganic reactive gaseous mercury in ambient air. Environ Sci Technol 36:3000–3009. https://doi.org/10.1021/es015887t

Laudon H et al (2016) The role of biogeochemical hotspots, landscape heterogeneity, and hydrological connectivity for minimizing forestry effects on water quality. Ambio 45:152–162. https://doi.org/10.1007/s13280-015-0751-8

Laurén A et al (2008) Impacts of logging residue and stump removal on nitrogen export to a stream: a modelling approach. Scand J For Res 23:227–235. https://doi.org/10.1080/02827580802116184

Lenth RV (2020) Emmeans: estimated marginal means, aka least-squares means, 1.4.4 edn.

Leterme B, Blanc P, Jacques D (2014) A reactive transport model for mercury fate in soil—application to different anthropogenic pollution sources. Environ Sci Pollut R 21:12279–12293. https://doi.org/10.1007/s11356-014-3135-x

Masek JG et al (2011) Recent rates of forest harvest and conversion in North America. J Geophys Res 116:G00K03. https://doi.org/10.1029/2010jg001471

Mazur M, Mitchell CPJ, Eckley CS, Eggert SL, Kolka RK, Sebestyen SD, Swain EB (2014) Gaseous mercury fluxes from forest soils in response to forest harvesting intensity: a field manipulation experiment. Sci Total Environ 496:678–687. https://doi.org/10.1016/j.scitotenv.2014.06.058

McCarter CPR, Sebestyen SD, Eggert SL, Kolka RK, Mitchell CPJ (2020a) Changes in hillslope hydrology due to clearcutting and residual biomass removal. Hydrol Process 34:5354-5369. https://doi.org/10.1002/hyp.13948

McCarter CPR, Sebestyen SD, Eggert SL, Haynes K, Kolka R, Mitchell CPJ (2020b) Hydrological data and site feature information for a forest clearcutting and residual biomass removal study at the Marcell Experimental Forest. Forest Service Research Data Archive, Fort Collins. https://doi.org/10.2737/RDS-2020-0049

McCarter CPR et al (2021) Water chemistry data for a forest clearcutting and residual biomass removal study at the Marcell Experimental Forest. Service Research Data Archive, Fort Collins. https://doi.org/10.2737/RDS-2021-0007

McDonnell JJ (1990) A rationale for old water discharge through macropores in a steep, humid catchment. Water Resour Res 26:2821–2832. https://doi.org/10.1029/WR026i011p02821

Mercury Deposition Network, Site MN16 (2021) Mercury Deposition Network, Site MN16. Wisconsin State Laboratory of Hygiene. Retrieved from https://nadp.slh.wisc.edu/data/sites/siteDetails.aspx?net=MDN&id=MN16.

Miller CL, Southworth G, Brooks S, Liang L, Gu B (2009) Kinetic controls on the complexation between mercury and dissolved organic matter in a contaminated environment. Environ Sci Technol 43:8548–8553. https://doi.org/10.1021/es901891t

Mitchell CPJ, Branfireun BA, Kolka RK (2009) Methylmercury dynamics at the upland-peatland interface: topographic and hydrogeochemical controls. Water Resour Res 45:W02406. https://doi.org/10.1029/2008wr006832

National Trends Network, Site MN16 (2020) National Trends Network, Site MN16. Wisconsin State Laboratory of Hygiene. Retrieved from http://nadp.slh.wisc.edu/data/sites/siteDetails.aspx?net=NTN&id=MN16.

Noguchi S, Tsuboyama Y, Sidle RC, Hosoda I (2001) Subsurface runoff characteristics from a forest hillslope soil profile including macropores, Hitachi Ohta, Japan. Hydrol Process 15:2131–2149. https://doi.org/10.1002/hyp.278

Oni SK et al (2015) Local- and landscape-scale impacts of clearcuts and climate change on surface water dissolved organic carbon in boreal forests. J Geophys Res 120:2402–2426. https://doi.org/10.1002/2015jg003190

Osterwalder S, Bishop K, Alewell C, Fritsche J, Laudon H, Åkerblom S, Nilsson MB (2017) Mercury evasion from a boreal peatland shortens the timeline for recovery from legacy pollution. Sci Rep 7:16022. https://doi.org/10.1038/s41598-017-16141-7

Oswald CJ, Branfireun BA (2014) Antecedent moisture conditions control mercury and dissolved organic carbon concentration dynamics in a boreal headwater catchment. Water Resour Res 50:6610–6627. https://doi.org/10.1002/2013wr014736

Oswald CJ, Heyes A, Branfireun BA (2014) Fate and transport of ambient mercury and applied mercury isotope in terrestrial upland soils: insights from the METAALICUS watershed. Environ Sci Technol 48:1023–1031. https://doi.org/10.1021/es404260f

Pinel-Alloul B, Prepas E, Planas D, Steedman R, Charette T (2002) Watershed impacts of logging and wildfire: case studies in Canada. Lake Reserv Manag 18:307–318. https://doi.org/10.1080/07438140209353937

Pokharel AK, Obrist D (2011) Fate of mercury in tree litter during decomposition. Biogeosciences 8:2507–2521. https://doi.org/10.5194/bg-8-2507-2011

Pompeani DP, Cooke CA, Abbott MB, Drevnick PE (2018) Climate, fire, and vegetation mediate mercury delivery to midlatitude lakes over the holocene. Environ Sci Technol 52:8157–8164. https://doi.org/10.1021/acs.est.8b01523

Porvari P, Verta M, Munthe J, Haapanen M (2003) Forestry practices increase mercury and methyl mercury output from boreal forest catchments. Environ Sci Technol 37:2389–2393. https://doi.org/10.1021/es0340174

Pryor SC, Scavia D (2014) Midwest. In: Melilo JM, Richmon TC, Yohe GW (eds) Climate change impacts in the United States: the third national climate assessment. U.S. Global Change Research Program, Washington, DC, pp 418–440. https://doi.org/10.7930/J0J1012N

R Development Core Team (2021) R: A language and environment for statistical computing. R Foundation for Statistitical Computing, Vienna

Riscassi AL, Scanlon TM (2011) Controls on stream water dissolved mercury in three mid-Appalachian forested headwater catchments. Water Resour Res 47:W12512. https://doi.org/10.1029/2011wr010977

Schelker J, Eklöf K, Bishop K, Laudon H (2012) Effects of forestry operations on dissolved organic carbon concentrations and export in boreal first-order streams. J Geophys Res 117:G01011. https://doi.org/10.1029/2011jg001827

Sebestyen SD et al. (2020) Marcell experimental forest daily precipitation, 1961—ongoing, ver. 1 edn. USDA Forest Service, Environmental Data Initiative. https://doi.org/10.6073/pasta/75646a3bd41ba3219d0e578e8374eef7

Sebestyen S, Verry ES, Brooks K (2011) Hydrological responses to changes in forest cover on uplands and peatlands. In: Kolka RKS, Stephen D, Verry ES, Brooks KN (eds) Peatland biogeochemistry and watershed hydrology at the Marcell Experimental Forest. CRC Press, Boca Raton, pp 401–432

Sebestyen SD, Funke MM, Cotner JB, Larson JT, Aspelin NA (2017) Water chemistry data for studies of the biodegradability of dissolved organic matter in peatland catchments at the Marcell Experimental Forest: 2009–2011. Forest Service Research Data Archive, Fort Collins. https://doi.org/10.2737/RDS-2017-0067

Sebestyen SD, Funke MM, Cotner JB (2021a) Sources and biodegradability of dissolved organic matter in two peatland catchments with different upland forest types, northern Minnesota, USA. Hydrol Process 35:e14049. https://doi.org/10.1002/hyp.14049

Sebestyen SD, Lany NK, Roman DT, Burdick JM, Kyllander RL, Verry ES, Kolka RK (2021b) Hydrological and

meteorological data from research catchments at the Marcell Experimental Forest, Minnesota, USA. Hydrol Process 35:e14092. https://doi.org/10.1002/hyp.14092

Skyllberg U, Westin MB, Meili M, Björn E (2009) Elevated concentrations of methyl mercury in streams after forest clear-cut: a consequence of mobilization from soil or new methylation? Environ Sci Technol 43:8535–8541. https://doi.org/10.1021/es900996z

Sørensen R, Meili M, Lambertsson L, Cv B, Bishop K (2009) The effects of forest harvest operations on mercury and methylmercury in two boreal streams: relatively small changes in the first two years prior to site preparation. Ambio 38(364–372):369. https://doi.org/10.1579/0044-7447-38.7.364

Stewart-Oaten A, Murdoch WW, Parker KR (1986) Environmental impact assessment: "Pseudoreplication" in time? Ecology 67:929–940. https://doi.org/10.2307/1939815

Timmons DR, Verry ES, Burwell RE, Holt RF (1977) Nutrient transport in surface runoff and interflow from an aspen-birch forest. J Environ Qual 6:188–192. https://doi.org/10.2134/jeq1977.00472425000600020018x

Tjerngren I, Karlsson T, Björn E, Skyllberg U (2012) Potential Hg methylation and MeHg demethylation rates related to the nutrient status of different boreal wetlands. Biogeochemistry 108:335–350. https://doi.org/10.1007/s10533-011-9603-1

Tsuboyama Y, Sidle RC, Noguchi S, Hosoda I (1994) Flow and solute transport through the soil matrix and macropores of a hillslope segment. Water Resour Res 30:879–890. https://doi.org/10.1029/93WR03245

Ukonmaanaho L et al (2016) Impacts of forest harvesting on mobilization of Hg and MeHg in drained peatland forests on black schist or felsic bedrock. Environ Monit Assess 188:228. https://doi.org/10.1007/s10661-016-5210-x

United States Environmental Protection Agency (1996) Method 1669: sampling ambient water for determination of trace metals at water quality criteria levels vol EPA/821/R–96/011. United States Environmental Protection Agency, Washington, DC

Verry ES, Timmons DR (1982) Waterborne nutrient flow through an upland-peatland watershed in Minnesota. Ecology 63:1456–1467. https://doi.org/10.2307/1938872

Verry ES, Brooks KN, Nicholas DS, Ferris DR, Sebestyen SD (2011) Watershed hydrology. In: Kolka RK, Sebestyen S, Verry ES, Brooks K (eds) Peatland biogeochemistry and watershed hydrology at the Marcell Experimental Forest. CRC Press, Boca Raton, pp 193–212

Verry ES, Elling AE, Sebestyen SD, Kolka RK, Kyllander R (2018) Marcell experimental forest daily streamflow data. Forest Service Research Data Archive, Fort Collins. https://doi.org/10.2737/RDS-2018-0009

Weiler M, McDonnell J (2004) Virtual experiments: a new approach for improving process conceptualization in hillslope hydrology. J Hydrol 285:3–18. https://doi.org/10.1016/S0022-1694(03)00271-3

Weiler M, McDonnell JJ (2007) Conceptualizing lateral preferential flow and flow networks and simulating the effects on gauged and ungauged hillslopes. Water Resour Res 43:W03403. https://doi.org/10.1029/2006wr004867

Woerndle GE, Tsz-Ki Tsui M, Sebestyen SD, Blum JD, Nie X, Kolka RK (2018) New insights on ecosystem mercury cycling revealed by stable isotopes of mercury in water flowing from a headwater peatland catchment. Environ Sci Technol 52:1854–1861. https://doi.org/10.1021/acs.est.7b04449

Zhou J, Obrist D, Dastoor A, Jiskra M, Ryjkov A (2021) Vegetation uptake of mercury and impacts on global cycling. Nat Rev Earth Environ 2:269–284. https://doi.org/10.1038/s43017-021-00146-y